

Properties of some ferrocene macrocyclic dioxotetraamines: the roles of aromatic side-arms

Peng Xue, Quan Yuan, Enqin Fu *, Chengtai Wu

Department of Chemistry, Wuhan University, Wuhan 430072, China

Received 5 January 2001; received in revised form 9 April 2001; accepted 10 April 2001

Abstract

The coordination chemistry and electrochemical behavior of a series of ferrocene macrocyclic dioxotetraamines **1–4** each of which bears a pendant aromatic group and a malonic diamide fragment in their framework were investigated by electronic absorption spectroscopy and cyclic voltammetry. For the purpose of comparison, their model compounds **5–8** were also synthesized and studied. The stoichiometry of 1:1 for the complexes has been confirmed by FAB mass spectroscopy and UV–vis titration of Cu(II) ion with ligands **4** and **8**. Stability constants for the equilibrium of the above complexes have been evaluated. The ferrocene ligands **1–4** can electrochemically recognize the transition metal ions (Co^{2+} , Ni^{2+} and Cu^{2+}), while those ligands with a complexible atom in the side-arm can stabilize selectively the uncommon state of Ni(III). © 2001 Elsevier Science B.V. All rights reserved.

Keywords: Ferrocene; Macrocyclic polyamine; Synthesis; Coordination; UV–vis spectrometry; Cyclic voltammetry

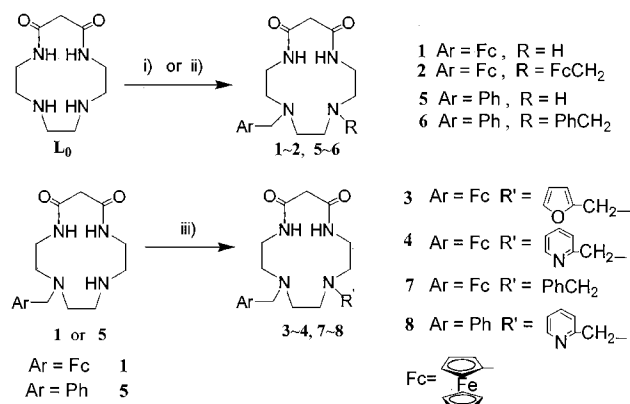
1. Introduction

In the past two decades, a large number of redox-active host molecules have been synthesized with the hope that they may be used as chemosensors [1,2], redox-switchable ligands [3] or redox catalysts [4].

Among these compounds, ferrocene macrocyclic polyamines have shown some interesting behavior due to their redox activity and complexibility toward transition metal ions and anions [5]. On the other hand, the macrocyclic dioxopolyamines possess the unique dual structural features of saturated macrocyclic polyamines and oligopeptides and show some interesting coordination behavior [6,7]. Recently, we have reported that the ferrocene macrocyclic dioxopolyamines which bear iminodiacetamide in the framework of their rings can electrochemically recognize the cations such as Co^{2+} , Ni^{2+} and Cu^{2+} , and selectively stabilize the uncommon state of Ni^{3+} or Cu^{3+} . Particularly interesting is

the fact that this selectivity is ring-size-dependent [8].

In order to investigate the side-arm effect in this type of ligands on stabilizing the trivalent state of these cations, we have synthesized recently the ferrocene macrocyclic dioxotetraamines which bear a pendant pyridine, furan or ferrocene (**1–4**) [9]. For the purpose



i) $\text{FcCH}_2\text{NMe}_3\text{I}$, EtOH, K_2CO_3 , reflux, ii) PhCH_2Cl , EtOH, K_2CO_3 , reflux, iii) $\text{R}'\text{Cl}$, CH_3CN , K_2CO_3 , reflux,

Scheme 1.

* Corresponding author. Tel.: +86-27-87684117; fax: +86-27-87647617.

E-mail address: jgqin@whu.edu.cn (E. Fu).

of comparison, model compounds **5–8**, which were not reported before, were also synthesized (Scheme 1). Phenyl was chosen in the model compounds as the substitute for the reason that it exhibits the aromaticity similar to pyridine, furan and ferrocene but without the complexible atom or redox activity. In this paper, the synthesis of compounds **5–8** and some coordination compounds of **1** and **2** are presented, and FABMS, UV–vis spectroscopy, and cyclic voltammetry (CV) are employed to investigate the coordination chemistry and the electrochemical behavior of compounds **1–8**.

2. Experimental

2.1. General

4-Ferrocenylmethyl-1,4,7,10-tetraaza-cyclotridecane-11,13-dione (**1**), 4,7-bis(ferrocenylmethyl)-1,4,7,10-tetraaza-cyclotridecane-11,13-dione (**2**), 4-ferrocenylmethyl-7-furfuryl-1,4,7,10-tetraaza-cyclotridecane-11,13-dione (**3**), 4-ferrocenylmethyl-7-picolyl-1,4,7,10-tetraaza-cyclotridecane-11,13-dione (**4**) were prepared according to the method in our previous report [9]. Picolyl chloride was prepared according to a procedure in the literature [10]. The solvents used for the reaction were thoroughly dried analytical reagents. All melting points (m.p.) are uncorrected. IR spectra were obtained on a Nicolet 170SX FT-IR or Shimadzu FT-IR 8000 spectrophotometer. Proton magnetic resonance spectra (300 or 90 MHz) were recorded on a Varian Mercury-VX 300 or a JEOL FX90Q spectrometer with Me₄Si as internal reference. Mass spectra (FAB) were recorded on a ZAB 3F-HF spectrometer.

CV was performed in a conventional three-electrode cell at 20 ± 1 °C, using a PAR Model 173 potentiostat/galvanostat (EG&G), which was described in our previous report [8] except that the solvent was made of 2:1 (v/v) EtOH–H₂O.

UV–vis spectra were recorded on a Shimadzu UV-160A or UV-3100 spectrometer at 20 ± 1 °C in the mixture of 2:1 (v/v) EtOH–H₂O. The concentration of the ligands was always 1.0 mM for both UV–vis and electrochemical studies. The transition metal salts were used as in electrochemical experiments (the details can be found in the literature [7]). After the addition of metal ions, the solutions of the ligands were adjusted to pH 6–7 with NaOH (0.01 M).

2.2. Synthesis of ligands **5–8**

2.2.1. 4-Benzyl-1,4,7,10-tetraaza-cyclotridecane-11,13-dione (**5**) and 4,7-bis(benzyl)-1,4,7,10-tetraaza-cyclotridecane-11,13-dione (**6**)

1,4,7,10-Tetraaza-cyclotridecane-11,13-dione (**L**₀) (1.50 g, 7.0 mmol) was dissolved in 40 ml of absolute

EtOH, to which a solution of benzyl chloride (0.60 g, 5.0 mmol) in EtOH (40 ml) was added in drops under reflux. After the addition, 0.40 g (2.9 mmol) of K₂CO₃ was added and the mixture was heated under reflux for an additional hour. After the solvent was evaporated under reduced pressure, the residue was taken up in CHCl₃, and washed with water. The organic layer was separated, dried over anhydrous Na₂SO₄, filtered and concentrated under reduced pressure. The residue was separated by column chromatography on silica. Compound **6** was eluted by a mixture of CHCl₃ and MeOH (100:3, v/v), and purified by crystallization from Me₂CO. Yield: 0.30 g (15%), m.p. 150–152 °C. FABMS (exact mass, 394.24, *m/z*, %): 395 [M⁺ + 1, 77]; 394 [M⁺, 9]; 303 [M⁺ – 91, 42]; 91 [C₇H₇⁺, 100]. ¹H-NMR (CDCl₃, 90 MHz, δ ppm): 2.24–2.54 (m, 8H, CH₂NCH₂CH₂NCH₂); 3.26 (s, 2H, COCH₂CO); 3.28–3.40 (m, 4H, CONCH₂); 3.50 (s, 4H, PhCH₂N); 6.64–6.94 (s, br, 2H, CONH); 7.08–7.40 (m, 10H, C₆H₅). IR (KBr pellet, cm⁻¹): 3303 (s, of CONH); 3121 (m, of aryl); 2928, 2833 (m, of alkyl); 1668, 1634 (s, of CONH); 1535, 1550 (s, of CONH); 734 (m, mono-substituted phenyl); 698 (m, mono-substituted phenyl).

The mixture of CHCl₃ and MeOH (100:5–8, v/v) eluted compound **5**, which was purified by crystallization from Me₂CO. Yield: 0.91 g (60%), m.p. 204–206 °C. FABMS (exact mass, 304.19, *m/z*, %): 305 [M⁺ + 1, 100]; 304 [M⁺, 8]; 213 [M⁺ – 91, 5]; 91 [C₇H₇⁺, 80]. ¹H-NMR (CDCl₃, 90 MHz δ ppm): 2.20 (s, 1H, CNHC); 2.40–2.76 (m, 8H, CH₂NCH₂CH₂NCH₂); 3.22 (s, 2H, COCH₂CO); 3.24–3.50 (m, 4H, CONCH₂); 3.60 (s, 4H, PhCH₂N); 7.04–7.16 (m, 6H, CONH, C₆H₁₁); 8.00–8.24 (br, 1H, CONH). IR (KBr pellet, cm⁻¹): 3311, 3257 (m, of CONH); 3171 (m, of CNHC); 3125 (m, of aryl); 2940, 2831 (m, of alkyl); 1686, 1658 (s, of CONH); 1649, 1462 (m, of aryl); 1547 (s, of CONH); 769 (m, mono-substituted phenyl); 694 (m, mono-substituted phenyl).

2.2.2. 4-Benzyl-7-ferrocenylmethyl-1,4,7,10-tetraaza-cyclotridecane-11,13-dione (**7**)

To a mixture of compound **1** (0.20 g, 0.48 mmol) and K₂CO₃ (0.55 g, 4.0 mmol) in MeCN (10 ml), a solution of benzyl chloride (0.070 g, 0.55 mmol) in MeCN (5 ml) was added under reflux with stirring, the reaction was monitored by TLC. After being heated under reflux for 18 h, the reactant mixture was worked-up as described above, and separated by column chromatography on alumina (100:2, CHCl₃–MeOH, v/v), crystallization from MeCN afforded an orange powder. Yield: 0.15 g (62%), m.p. 152–154 °C. FABMS (exact mass, 502.20, *m/z*, %): 503 [M⁺ + 1, 27]; 502 [M⁺, 35]; 359 [M⁺ – 199 + 56, 5]; 303 [M⁺ – 199, 28]; 212 [M⁺ – 199 – 91, 3]; 199 [C₅H₅FeC₅H₄CH₂⁺, 100]; 91 [C₇H₇⁺, 60]. ¹H-NMR (CDCl₃, 300 MHz, δ ppm): 2.31–2.49 (m, 8H, CH₂NCH₂CH₂NCH₂); 3.26 (s); 3.35–3.37 (m); 3.52 (s)

(10H, COCH₂CO, CONCH₂, FeCH₂N, PhCH₂N); 3.94–3.96, 4.05–4.11 (d, t, 9H, C₅H₅FeC₅H₄); 6.70, 7.03 (br, br, 2H, CONH); 7.28–7.34 (m, 5H, C₆H₅). IR (KBr pellet, cm⁻¹): 3429, 3315 (m-s, of CONH); 3128 (s, of phenyl); 2920, 2860 (m, of alkyl); 1674, 1647 (s, of CONH); 1533 (s, of phenyl); 1549 (s, of CONH); 1101, 1000 (m, of ferrocenyl); 736, 710 (m, mono-substituted phenyl).

2.2.3. 4-Benzyl-7-(2-picolyl)-1,4,7,10-tetraaza-cyclotridecane-11,13-dione (**8**)

This compound was prepared following the same procedure as described for **7** except that column chromatography was carried out on silica (100:5, CHCl₃–MeOH, v/v), the compound was obtained as a viscous oil. Yield: 0.20 g (51%). FABMS (exact mass, 395.23, *m/z*, %): 396 [M⁺ + 1, 82]; 395 [M⁺, 17]; 304 [M⁺ – 91, 12]; 91 [C₇H₇⁺, 100]. ¹H-NMR (CDCl₃, 90 MHz, δ ppm): 2.28–2.60 (m, 8H, CH₂NCH₂CH₂NCH₂); 3.30, 3.12–3.46 (m, 6H, COCH₂CO, CONCH₂); 3.52 (s, 2H, PhCH₂N); 3.62 (s, 2H, NCH₂-pyridyl); 6.68–6.88 (m, 1H, 5-H of pyridyl); 7.04–7.32 (d, 6H, C₆H₅, 3-H of pyridyl); 7.48–7.72 (m, 1H, 4-H of pyridyl); 8.00–8.32 (m, 2H, CONH); 8.40–8.54 (m, 1H, 6-H of pyridyl). IR (KBr pellet, cm⁻¹): 3125 (s, of aryl); 2920, 2830 (m, of alkyl); 1665, 1650 (s, of CONH); 1549 (m-s, of CONH); 735, 700 (m, mono-substituted phenyl).

2.3. Preparation of the complexes

2.3.1. Copper(II) complex of **1**, [CuH₋₂L(**1**)]

The EtOH solution (20 ml) of **1** (0.20 g, 0.49 mmol) and Cu(OAc)₂·H₂O (0.10 g, 0.50 mmol) was heated to reflux under N₂ for 3 h. After the solution was concentrated under reduced pressure, crystallization from EtOH yielded black–purple needles. Yield: 0.15 g (65%). FABMS (exact mass, 473.08, *m/z*, %): 474 [M⁺ + 1, 48]; 473 [M⁺, 15]; 413 [(I)⁺ + 1, 5]; 199 [C₅H₅FeC₅H₄CH₂⁺, 100]. IR (KBr pellet, cm⁻¹): 3070 (m, of ferrocenyl); 2922, 2876 (m, of alkyl); 1622, 1600 (s, of CON⁻); 1091, 1005 (m, of ferrocenyl); 805 (m, of ferrocenyl). UV–vis: λ_{max} (nm) (ε, dm³ mol⁻¹ cm⁻¹): 451 (147).

2.3.2. Copper(II) complex of **2**, [CuH₋₂L(**2**)]

This compound was prepared following the same procedure as described for [CuH₋₂L(**1**)]. Recrystallization from MeOH–H₂O (1:2, v/v) afforded black–purple needles. FABMS (exact mass, 671.09, *m/z*, %): 672 [M⁺ + 1, 3]; 199 [C₅H₅FeC₅H₄CH₂⁺, 100]. IR (KBr pellet, cm⁻¹): 3079 (m, of ferrocenyl); 2931, 2866 (m, of alkyl); 1592, 1568 (s, of CON⁻); 1105, 1001 (m, of ferrocenyl); 798 (m, of ferrocenyl). UV–vis: λ_{max} (nm) (ε, dm³ mol⁻¹ cm⁻¹): 441 (334).

2.3.3. Nickel(II) complex of **2**, [NiH₋₂L(**2**)]

To the MeOH solution (6 ml) of **2** (0.305 g, 0.500 mmol) was added the aqueous solution (20 ml) of Ni(OAc)₂·4H₂O (124 mg, 0.500 mmol). The mixture was heated to 50–60 °C, and its pH value was adjusted to ca. 9 with NaOH. After being heated for 20 min, the mixture was filtered and cooled in a refrigerator, and red–orange crystals were obtained. Yield: 0.11 g (33%). FABMS (exact mass, 666.09, *m/z*, %): 667 [M⁺ + 1, 22]; 666 [M⁺, 7]; 199 [C₅H₅FeC₅H₄CH₂⁺, 100]. IR (KBr pellet, cm⁻¹): 3078 (m, of ferrocenyl); 2923, 2868 (m, of alkyl); 1585, 1566 (s, of CON⁻); 1104, 999 (m, of ferrocenyl); 806 (m, of ferrocenyl). UV–vis: λ_{max} (nm) (ε, dm³ mol⁻¹ cm⁻¹): 450 (357), 323 (488).

2.3.4. Cobalt(II) complex of **2**, [CoH₋₂L(**2**)]

This complex was prepared following the same procedure as described for [NiH₋₂L(**2**)] except that the pH value was not adjusted and MeOH was replaced by MeCN, black–purple crystals were obtained. FABMS (exact mass, 667.09, *m/z*, %): 668 [M⁺ + 1, 4]; 667 [M⁺, 5]; 199 [C₅H₅FeC₅H₄CH₂⁺, 100]. IR (KBr pellet, cm⁻¹): 3070 (m, of ferrocenyl); 2926, 2870 (m, of alkyl); 1588 (s, of CON⁻); 1104, 999 (m, of ferrocenyl); 806 (m, of ferrocenyl). UV–vis: λ_{max} (nm) (ε, dm³ mol⁻¹ cm⁻¹): 554 (264), 373 (850).

3. Results and discussion

Compounds **1–8** were prepared following the procedure shown in Scheme 1.

3.1. Coordination of compounds **1–8** with Ni²⁺, Co²⁺ and Cu²⁺ ions

IR, UV–vis spectra and FABMS data of all the complexes prepared confirmed the coordination between the transition metal ions and the macrocyclic ligands. Their IR spectra showed changes [8,11] in stretching vibration of both C=O (i.e. from 1670–1630 to 1620–1570 cm⁻¹) and N–H (disappeared in the complexes) in amide moieties. FABMS also showed the molecular ion peaks of MH₋₂L.

The addition of Ni²⁺ ion to the solutions of those ligands bearing ferrocene (i.e. **1–4**, **7**) usually did not cause obvious effect on the shifts in λ_{max} of ferrocene, but caused some changes in the extinction coefficient of ferrocene (except in the case of **7** and Ni²⁺) (Table 1). The addition of Cu²⁺ and Co²⁺ ions usually caused the shifts in λ_{max} and an increase in absorbance of ferrocene. However, in the case of those ligands bearing no ferrocene (i.e. **5**, **6**, **8**), the absorption peaks for all the central ions Ni²⁺, Cu²⁺ and Co²⁺ in the complexes showed distinctly (Fig. 1) that the extinction coefficients of the central cations increased in compari-

Table 1
The values of λ_{\max} (nm) and ϵ ($\text{mol}^{-1} \text{dm}^3 \text{cm}^{-1}$) for ligands **1–8** and their complexes

| | Ligand | In the presence of M^{2+} | | | |
|----------|------------------------------|------------------------------------|------------------------|------------------------|------------------------|
| | | Ni^{2+} | Cu^{2+} | Co^{2+} | |
| 1 | λ_1 (ϵ_1) | 436 (115) | 430 (231) | 412 (143) ^a | 363 (887) |
| | λ_2 (ϵ_2) | 325 (93) | 315 (334) | 665 (22) | 557 (279) |
| 2 | λ_1 (ϵ_1) | 438, 0.115 ^b | 450 (357) ^c | 441 (334) ^c | 373 (850) ^c |
| | λ_2 (ϵ_2) | 325, 0.082 | 323 (488) | | 554 (264) |
| 3 | λ_1 (ϵ_1) | 435 (105) | 433 (107) | 448 (201) | 433 (120) |
| | λ_2 (ϵ_2) | 323 (87) | 324 (103) | 524 (172) | 589 (21) ^d |
| 4 | λ_1 (ϵ_1) | 432 (126) | 429 (181) | 402 (230) | 417 (389) |
| | λ_2 (ϵ_2) | 320 (155) | 315 (297) | 595 (207) | |
| 5 | λ (ϵ) | | 387 (78) | 522 (119) | 585 (96) |
| 6 | λ_1 (ϵ_1) | | 382 (65) | 528 (34) | 590 (10) |
| | λ_2 (ϵ_2) | | | | 634 (10) |
| 7 | λ_1 (ϵ_1) | 434 (114) | 435 (111) | 413 (149) | 428 (154) |
| | λ_2 (ϵ_2) | 322 (89) | 324 (84) | 657 (28) | 311 (217) ^e |
| 8 | λ_1 (ϵ_1) | | 462 (152) | 601 (182) | 462 (599) |
| | λ_2 (ϵ_2) | | | | 635 (89) |

^a For the prepared complex, at 451 nm (ϵ , 147).

^b Absorbance of its saturated solution.

^c Of the prepared complex.

^d Another at 638 nm (ϵ , 20).

^e The others at 591 nm (ϵ , 39); 639 nm (ϵ , 39).

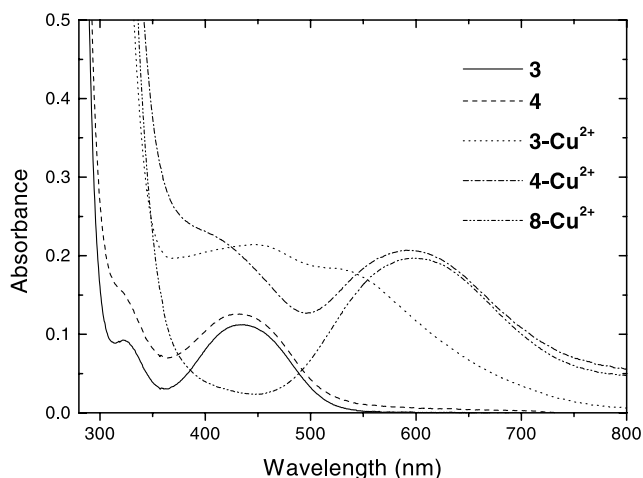


Fig. 1. UV-vis spectra of ligands **3**, **4**, **8** before and after addition of Cu^{2+} ion.

son with the hydrated ions. All these evidences showed the occurrence of interaction between ligands **1–8** and the metal ions mentioned above.

For model compounds **5–8**, the extinction coefficients for each central metal ion have remarkable differences. The approximate order $\mathbf{8} > \mathbf{5} > \mathbf{7} \cong \mathbf{6}$ for nearly all these metal ions may reflect the order of coordination ability of these ligands. It may be concluded that the coordination ability was enhanced by the side-arm with a complexible atom while it reduced for the side-arm without one.

The increase in absorbance at λ_{\max} for the copper complexes of ligands **4** and **8** upon incremental addition of Cu^{2+} ion are given in Table 2, the data are illustrated in Fig. 2. The progressive increase in absorbance intercepted the limiting ‘infinity’ absorbance both at molar ratio 1.1:1 of Cu^{2+} to ligands **4** or **8**. Therefore the complexation stoichiometry for the complexes is 1:1. The equilibrium constants were evaluated by the plot of $1/\Delta A$ against $1/[\text{M}]$ based on the Benesi–Hildebrand equation [12] to obtain the values for bimolecular equilibrium constants of 161 (Cu^{2+} –**4**), 100 (Cu^{2+} –**8**) $\text{mol}^{-1} \text{dm}^3$.

3.2. Electrochemical behavior of compounds **1–8**

Some of the cyclic voltammograms for the ligands before and after addition of Ni^{2+} , Co^{2+} and Cu^{2+} metal ions were chosen and are shown in Figs. 3–5. The peak potentials (E values vs. SCE) of each couple for all the ligands and their complexes are summarized in Tables 3 and 4.

The redox peaks separations (66–92 mV) of most couples (Tables 3 and 4) indicated the quasi-reversible redox process for these ligands and their complexes. Some couples are reversible (e.g. an oxidation peak at 407 mV for the nickel(II) complex of **4**, an oxidation peak at 423 mV for ligand **3** at pH 7, etc.), and some are irreversible (e.g. an oxidation peak at 415 mV for the cobalt(II) complex of **1**, 644 mV for the copper(II) complex of **5**, etc.). The wider potential peaks’ separation between the anodic and the cathodic peaks suggests a stronger interaction between the metal ion and the ferrocene subunit, because the electrostatic interaction makes the oxidation of ferrocene less favorable (which results in the anodic shift in the oxidation peak potential) and is in favor of the reduction of ferrocenium (which leads to the cathodic shift in the reduction peak potential).

In order to investigate how the pH values of solutions affect the redox peak potentials of ferrocene in the ligands, the electrochemical behavior of these ligands have been investigated under different pH values. It was observed that a decrease in the pH value results in an increase in the oxidation peak potential of ferrocene (Table 3, Fig. 3). A lower pH value favors the protonation of amines of macrocyclic polyamines, the electrostatic repulsion between protonated amine and ferrocenium cation have made the oxidation of ferrocene more difficult; as a result, the oxidation potential of ferrocene is higher in the solution of lower pH values.

Maybe there are different species in the solution of **2–4** at pH 3–5, 7, 7, respectively, and in the complex solution of **1** ($\text{Ni}(\text{II})$, $\text{Co}(\text{II})$, $\text{Cu}(\text{II})$), **3** ($\text{Cu}(\text{II})$), **4** ($\text{Ni}(\text{II})$), because more than two redox peaks were observed (Tables 3 and 4).

Table 2
Absorption data at complex λ_{\max} for solution of ligands **4** (1 mM) and **8** (1 mM) upon incremental molar ratio addition of Cu^{2+}

| Cu^{2+} - 4 | <i>A</i> | Cu^{2+} - 4 | <i>A</i> | Cu^{2+} - 8 | <i>A</i> | Cu^{2+} - 8 | <i>A</i> |
|-----------------------------|----------|-----------------------------|----------|-----------------------------|----------|-----------------------------|----------|
| 0 | 0.000 | 1.1 | 0.248 | 0 | 0.0028 | 1.0 | 0.2086 |
| 0.10 | 0.026 | 1.2 | 0.253 | 0.10 | 0.0204 | 1.1 | 0.2302 |
| 0.20 | 0.039 | 1.3 | 0.260 | 0.20 | 0.0415 | 1.2 | 0.2347 |
| 0.30 | 0.072 | 1.4 | 0.265 | 0.30 | 0.0610 | 1.3 | 0.2411 |
| 0.40 | 0.095 | 1.5 | 0.276 | 0.40 | 0.0868 | 1.4 | 0.2517 |
| 0.50 | 0.122 | 1.6 | 0.280 | 0.50 | 0.1051 | 1.5 | 0.2576 |
| 0.60 | 0.145 | 1.8 | 0.288 | 0.60 | 0.1250 | 1.6 | 0.2515 |
| 0.70 | 0.171 | 2.0 | 0.296 | 0.70 | 0.1526 | 2.0 | 0.2655 |
| 0.80 | 0.196 | 2.5 | 0.302 | 0.80 | 0.1725 | 2.4 | 0.2611 |
| 0.90 | 0.216 | 3.0 | 0.302 | 0.90 | 0.1971 | 3.0 | 0.2603 |
| 1.0 | 0.237 | | | | | | |

Compared with the free ligands **1**, **2**, **4** (at pH 7), the addition (1:1, molar ratio) of each of the transition metal ions Cu(II), Ni(II), Co(II) has caused significant shifts in the oxidation peak potentials for the corresponding Fc^+/Fc couple to the more anodic direction. The largest shifts for **1**, **2** and **4** were caused by copper(II) ($\Delta E_{\text{pa}} = 147$ mV), nickel(II) ($\Delta E_{\text{pa}} = 104$ mV) and cobalt(II) ($\Delta E_{\text{pa}} = 75$ mV) ions, respectively. Further addition (2:1, 3:1, molar ratio) of these metal ions afforded almost the same results. The ΔE_{pa} values show the difference between the potentials of Fc^+/Fc in the complexed ($E_{\text{pa,c}}$) and free ($E_{\text{pa,f}}$) ligands (Table 4). No obvious shift in potential was observed after the addition of these metal ions to the electrochemical solution of the model compound **7**. One of the reasons may be short-time reaction with the metal ions; another is its weaker coordination ability compared with ligand **1**.

It should be noticed that ligands **3**, **4** and **8** which bear a side-arm with a complexible atom can stabilize selectively the uncommon state of Ni(III) ion, which is different from the reported results of stabilization of both Ni(III) and Cu(III) ions [13]. While those bearing a side-arm with no complexible atom such as ligands **1**, **2**, **6**, **7** did not show such an ability. Ligand **5** can stabilize selectively Cu(III) ion instead, although it is irreversible (Table 4).

The selective stabilization of Cu(III) or Ni(III) may be associated with the following factors [7]: (i) the ring size of macrocycle, (ii) the ionic radii of the two metal ions in different oxidation states, and (iii) the coordination configuration which depends on the ligand field strength and the electronic states of metal cations.

Due to the strong co-planarity caused by the conjugated imide anions after coordination, the dioxo [13] aneN_4 (L_0) yields the square-planar low-spin Ni(II) complex [6,14]. The ideal M–N bond length for fitting into the cavity of the coplanar **3**, **4** or **8** (~ 1.92 Å) is not prohibitively short for the low-spin Ni(II) (Ni(II)–N average bond length is equal to 1.88 Å [10], 1.89 Å [14,15]). Actually the N,N' -di-substituted dioxo

[13] aneN_4 is just fit to this cation according to the structure determined by X-ray crystallography [11]. But the low-spin d^7 Ni(III) (Ni(III)–N bond length is equal to 1.97 Å [16]) would possess longer bond distance with N atom than the low-spin d^8 Ni(II). Moreover, the low-spin d^7 Ni(III) prefers an axial coordination; therefore, the uncommon Ni(III) has to rise from the plane

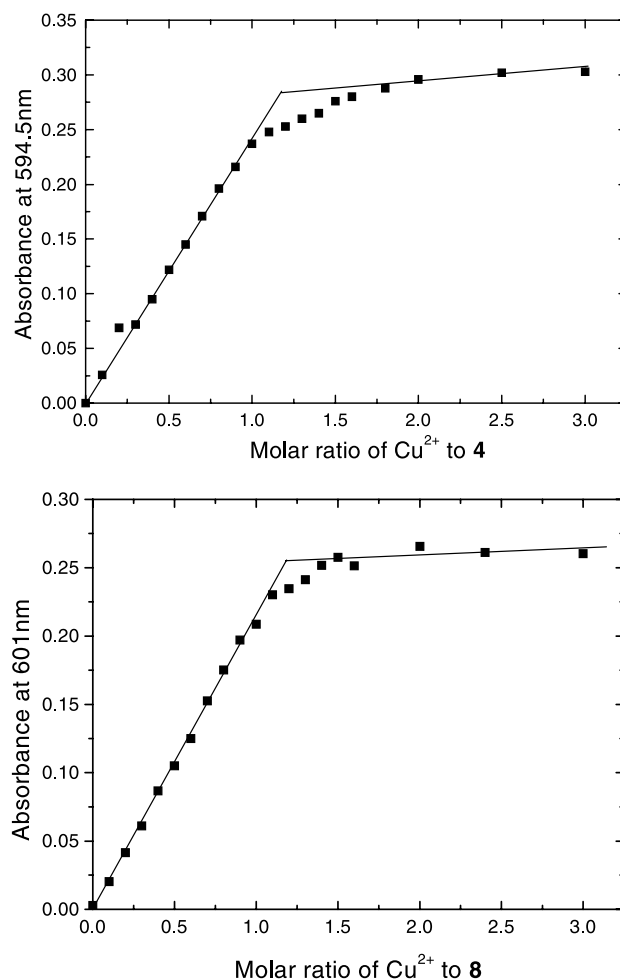


Fig. 2. Plots of A_{\max} vs. molar ratio of Cu^{2+} ion to ligands **4** and **8**.

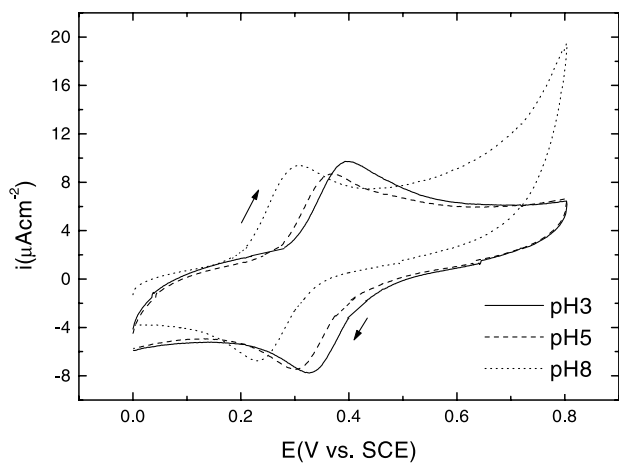


Fig. 3. Cyclic voltammograms of ligand **1** in different pH values.

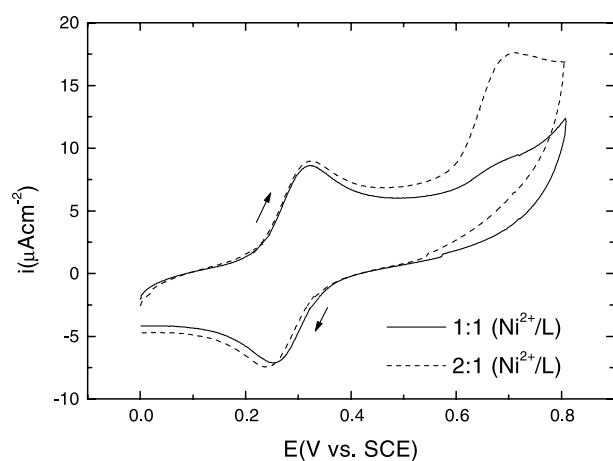


Fig. 4. Cyclic voltammograms of ligand **3** in the presence of Ni²⁺ ion.

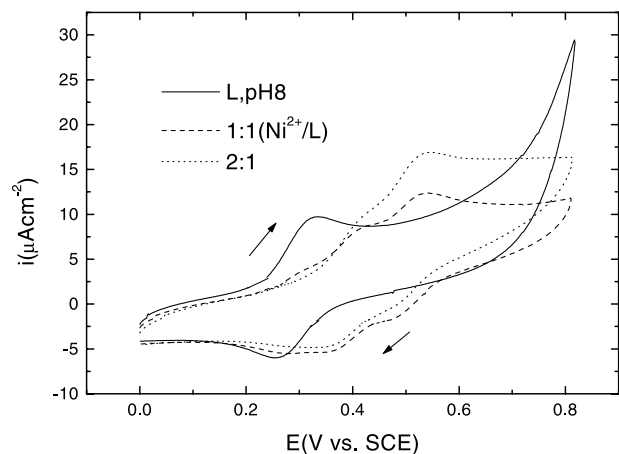


Fig. 5. Cyclic voltammograms of ligand **4** in the presence or absence of Ni²⁺ ion.

of the four N's ring while Ni(II) is oxidized. The axial coordination by the nitrogen or the oxygen of pyridine or furan in the side-arm will help the metal

ion to rise. So the oxidation of Ni(II) becomes easier and the oxidation peak potential occurred at a lower position (**3**, $E_{pa} = 717$ mV; **4**, $E_{pa} = 542$ mV; **8**, $E_{pa} = 540$ mV) than that with no side-arm (**L**₀, $E^{\circ} = 0.92$ V [6]). To some extent, the reason for those without a complexible atom in the side-arm exhibiting no evidences of stabilization of Ni(III) in the potential range tested is that they have no atom for axial coordination.

On the other hand, the ring sizes of the coplanar ligand **3**, **4**, **8** are short for the Cu(II)–N bond length (average value is 1.98–2.00 Å [17], 2.03 Å [6,14]), so that the metal ion Cu(II) has to stay above the coplanar N₄. The change of Cu(II) to Cu(III) (d⁸, low-spin) will drastically reduce (0.12–0.17 Å) the ionic radius of the metal [18]; as a result, Cu(III) tends to fall into the cavity of the macrocycle without an axial coordination. However, the axial coordination will prevent the cation from falling while it is oxidized, so the oxidation peak potential will shift toward the more anodic direction, in our experiment it did not appear in the scan range. Without these disadvantages, the model compound **5** exhibits the oxidation peak at 644 mV for Cu(III)H₋₂L/Cu(II)H₋₂L. Model compounds **6** and **7** do not exhibit this property as compound **5** does. This may due to its weak coordination described in Section 3.1. The reason for the ferrocene macrocycle **1** not to exhibit this property may be the effect of ferrocene adjacent to the copper ion, and this will be discussed in another paper.

These results are in good agreement with that reported in our previous paper [8] about ferrocene macrocyclic polyamines bearing iminodiacetamides. Kimura [13] has investigated the effect of the side-arm attached to some dioxo-polyamines on stabilizing Ni(III), Cu(III). The trend he found is in coincidence with our work, but the results indicated that our compounds exhibited higher selectivity under our experimental conditions.

4. Conclusions

Cyclic voltammetry revealed that a decrease in the pH value of the solution results in an increase in the oxidation peak potential of ferrocene in ligands **1**–**4**. The ferrocene ligands can electrochemically recognize the transition metal ions, Co(II), Ni(II) and Cu(II), while an uncommon state of Ni(III) can be stabilized selectively by ligands **3**, **4** and **8** which bear a side-arm with a complexible atom. Electronic absorption spectroscopy identified that the interaction between the ligands and the transition metal ions has an effect on d–d transition of ferrocene and the guest cation. The complexible atom in the side-arm plays an im-

portant role in selective stabilization of the trivalent state of Ni(III) and in the complexibility of a ligand. The complexation stoichiometry 1:1 ($M^{2+} - L$) for the

complexes were verified by FABMS of the complexes and UV–vis titration. The equilibrium constants for the copper complexes of **4** and **8** were evaluated.

Table 3
The E values for ligands **1–4**, **7** in the solutions of different pH values

| pH | | 3 | 4 | 5 | 6 | 7 | 8 | 9 |
|----|------------------------------|------------------------|------------------|----------------------|------------------|----------------------|----------|------------------|
| 1 | E_{pa} (mV) | 400 | 382 | 373 | | 328 | 308 | 308 |
| | E_{pc} (mV) | 328 | 315 | 299 | | 254 | 231 | 229 |
| | ΔE (mV) ^a | 72 | 67 | 74 | | 74 | 77 | 79 |
| 2 | E_{pa} (mV) | 388/502 ^{b,c} | | 384/504 ^c | | 345 | 328 | |
| | E_{pc} (mV) | 324/440 | | 317/438 | | 293 | 260 | |
| | ΔE (mV) | 64/62 | | 67/66 | | 52 | 68 | |
| 3 | E_{pa} (mV) | | 435 ^d | | | 336/423 ^c | | 328 ^e |
| | E_{pc} (mV) | | 361 | | | 270/375 | | 247 |
| | ΔE (mV) | | 74 | | | 66/48 | | 81 |
| 4 | E_{pa} (mV) | 485 | | | 457 ^f | 345/407 ^c | | 337 ^e |
| | E_{pc} (mV) | 419 | | | 387 | 273/375 | | 255 |
| | ΔE (mV) | 66 | | | 70 | 72/32 | | 82 |
| 7 | E_{pa} (mV) | | | 408 | | 340 | | 332 ^e |
| | E_{pc} (mV) | | | 342 | | 269 | | 257 |
| | ΔE (mV) | | | 66 | | 71 | | 75 |

^a Redox peaks separation $\Delta E = E_{pa} - E_{pc}$, error of E values, ± 5 mV.

^b pH 3–4.

^c Relative to Fc^+/Fc of protonated species.

^d pH 4–5.

^e pH 8–9.

^f pH 5–6.

^g pH 9–10.

Table 4
The E values for ligands **1–5**, **7**, **8** before and after addition of metal ions^a

| Complex/ligand | Nil | Ni^{2+} | Cu^{2+} | Co^{2+} | |
|----------------|-----------------------------------|-----------|------------------------------------------------------|------------------------------------|--------------|
| 1 | E_{pa} (mV) | 328 | 312/424 | 375/475 | 313/415 |
| | E_{pc} (mV) | 254 | 233 | 243/338 | 232 |
| | ΔE_{pa} (mV) ^b | | –16/96 | 47/147 | –15/87 |
| 2 | E_{pa} (mV) | 345 | 449 | 400 | 412 |
| | E_{pc} (mV) | 293 | 383 | 341 | 345 |
| | ΔE_{pa} (mV) | | 104 | 55 | 67 |
| 3 | E_{pa} (mV) | 336/423 | 328 ^c /717 ^d | 335 ^c /392 ^f | 331 |
| | E_{pc} (mV) | 270/375 | 256 | 270 | 258 |
| | ΔE_{pa} (mV) | | ^g | 57 | ^g |
| 4 | E_{pa} (mV) | 345/407 | 337 ^c /427 ^c /542 ^d | 409 | 420 |
| | E_{pc} (mV) | 273/375 | 278/356/468 | 330 | 356/275 |
| | ΔE_{pa} (mV) | | ^g /20 | 64 | 75 |
| 5 | E_{pa} (mV) | | | 644 ^h | |
| | E_{pc} (mV) | | | | |
| 7 | E_{pa} (mV) | 340 | 339 | 332 | 332 |
| | E_{pc} (mV) | 269 | 264 | 258 | 262 |
| | ΔE (mV) | | ^g | ^g | ^g |
| 8 | E_{pa} (mV) | | 540 ^d | | |
| | E_{pc} (mV) | | 454 | | |

^a All the experiments were carried out at the pH value of ca. 7 (no buffer).

^b $\Delta E_{pa} = E_{pa,c} - E_{pa,f}$, error of E values, ± 5 mV.

^c Relative to Fc^+/Fc .

^d Relative to $Ni(III)H_{-2}L/Ni(II)H_{-2}L$ couple.

^e Relative to Fc^+/Fc of uncomplexed species.

^f Relative to Fc^+/Fc of complex.

^g The absolute values are not more than 10 mV.

^h Relative to $Cu(III)H_{-2}L/Cu(II)H_{-2}L$ couple, irreversible.

Molecular systems capable of controlling redox properties of metal ions are of interest in such fields as catalysis and electrocatalysis [19], in which some application may be found on the basis of the results of the electrochemical study of these compounds. Besides, the ferrocene ligands **1–4** may find application in electrochemical sensors.

Acknowledgements

The financial support from the National Natural Science Foundation of China and the kind supply of electrochemical instruments from Professor Fu-xing Gan of this University are gratefully acknowledged.

References

- [1] C.D. Hall, in: A. Togni, T. Hayashi (Eds.), *Ferrocenes*, VCH, Weinheim, 1995, p. 279 (and references therein).
- [2] P.D. Beer, *Adv. Inorg. Chem.* 39 (1992) 79 (and references therein).
- [3] A.E. Kaifer, S. Mendoza, in: G.W. Gokel (Ed.), *Comprehensive Supramolecular Chemistry*, vol. 1, Pergamon, Oxford, 1996, p. 701.
- [4] M.J.L. Tendero, A. Benito, J. Cano, J.M. Lloris, R. Martinez-Manez, J. Soto, A.J. Edwards, P.R. Raithby, A. Rennie, *J. Chem. Soc. Chem. Commun.* (1995) 1643.
- [5] P.D. Beer, Z. Chen, M.G.B. Drew, J. Kingston, M. Ogden, P. Spencer, *J. Chem. Soc. Chem. Commun.* (1993) 1046.
- [6] E. Kimura, in: S.R. Cooper (Ed.), *Crown Compounds: Toward Future Application*, VCH, Weinheim, 1992, p. 81.
- [7] E. Kimura, *J. Coord. Chem.* 15 (1986) 1.
- [8] P. Xue, E. Fu, M. Fang, C. Gao, C. Wu, *J. Organomet. Chem.* 598 (2000) 42.
- [9] P. Xue, E. Fu, G. Wang, C. Wu, *Synth. Commun.* 29 (1999) 1585.
- [10] J.F. Vozza, *J. Org. Chem.* 27 (1962) 3856.
- [11] X. Bu, D. An, Z. Zhu, Y. Chen, M. Shionoya, E. Kimura, *Polyhedron* 16 (1997) 179.
- [12] H.A. Benisi, J.H. Hildebrand, *J. Am. Chem. Soc.* 71 (1949) 2703.
- [13] E. Kimura, *Pure Appl. Chem.* 61 (1989) 823.
- [14] V.J. Thom, J.C.A. Boeyens, G.J. McDougall, R.D. Hancock, *J. Am. Chem. Soc.* 106 (1984) 3198.
- [15] M.F. Richardson, R.E. Sievers, *J. Am. Chem. Soc.* 94 (1972) 4134.
- [16] T. Ito, K. Sugimoto, H. Ito, *Chem. Lett.* (1981) 1477.
- [17] X. Bu, Z. Zhang, D. An, Y. Chen, M. Shionoya, E. Kimura, *Inorg. Chim. Acta* 249 (1996) 125.
- [18] L.L. Diaddari, W.R. Robinson, D.W. Margerum, *Inorg. Chem.* 22 (1983) 1021.
- [19] M.F. Richardson, R.E. Sievers, *J. Am. Chem. Soc.* 94 (1972) 4134.